VALIDATION OF MERIS REMOTE SENSING REFLECTANCE IN ATLANTIC CASE 1 WATERS WITH GROUND BASED IN-SITU MEASUREMENTS

Anja Theis[(1)], Bettina Schmitt[(1)], Steffen Gehnke[(2)], Roland Doerffer[(2)], Astrid Bracher[(1)]

[(1)]Alfred-Wegener-Institute, P.O box 120161, 27515 Bremerhaven, Germany, Email: Anja.Theis@awi.de
[(2)]GKSS Institute for Coastal Research, Max Planck-Straße 1, 21502 Geesthacht, Germany

ABSTRACT

In this paper MERIS remote sensing reflectances at sea surface for case 1 waters were validated with in-situ measurements. The in-situ data sets were collected during ship cruises across the Atlantic Ocean and taken with a system of three TriOS-RAMES hyperspectral spectroradiometers, measuring above-water upwelling radiance, downwelling irradiance and sky radiance. From these data sets, the water leaving remote sensing reflectance was calculated. Results will help to evaluate the atmospheric correction applied to MERIS case 1 data and are used to interpret the comparisons of in-situ measured chl a and MERIS algal-1 chl a.

1. INTRODUCTION

There are several studies about validation of MERIS products for case 2 waters but data concerning case 1 waters are scarce (e.g. [4]).

In this study three hyperspectral spectroradiometers measure above-water upwelling radiance, downwelling irradiance and sky radiance during different ship cruises across the Atlantic Ocean. From these data the in-situ water leaving remote sensing reflectance ρ_w is calculated in order to validate MERIS remote sensing reflectance ρ_m and to estimate errors in the MERIS case 1 water products. Since data evaluation is still going on, in this work we focus on only one of the cruises: ANT XXIV-4 with RV Polarstern in April and May 2008 from Chile to Germany.

2. MATERIALS AND METHODS

2.1. Instruments

The in-situ data were collected with three hyperspectral TriOS-RAMSES radiometers measuring:

- Downwelling irradiance E_d
- Sky radiance L_s at a zenith angle of 40° and an azimuth angle of 135°
- Upwelling radiance L_u at a nadir angle of 40° and the same azimuth angle as L_s

Fig. 1 and 2 show the instruments and an example of the measured spectra.

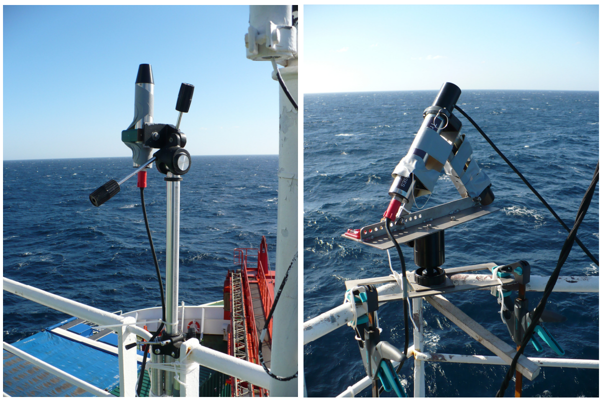

Figure 1. TriOS-RAMSES irradiance (left) and radiance (right) sensors mounted on board of RV Polarstern

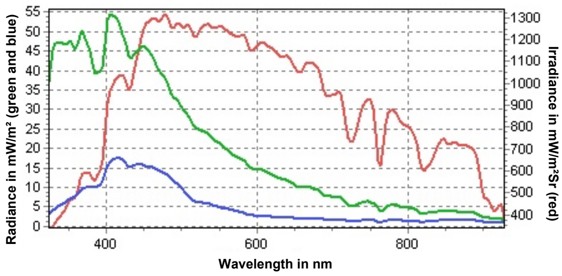

Figure 2. Example of the measured spectra (downwelling irradiance (red) in mW/m² Sr, sky radiance (green) and upwelling radiance (blue) in mW/m²)

All three devices have a spectral range of 320 nm to 950 nm and measure approximately every 3.3 nm. Their spectral width is about 10 nm and the field of view 7°.

2.2. Measurement methods

Measurements considered here were carried out during RV Polarstern cruise ANT XXIV-4 (April to May 2008) from Punta Arenas (Chile) to Bremerhaven (Germany) (Fig. 3). To minimize impacts from the ship shadow and reflection, the sensors were mounted in a steel frame as close to the bow of the ship as possible.

To prevent the interference of whitecaps, measurements were accomplished while ship was stationary.

Proc. of the '2nd MERIS / (A)ATSR User Workshop', Frascati, Italy
22–26 September 2008 (ESA SP-666, November 2008)

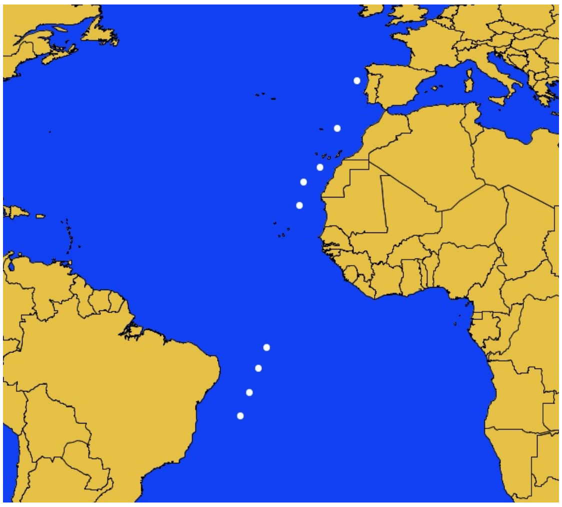

Figure 3. Sampling stations of measurement during ship cruise ANT_XXIV-4 from Chile to Germany

2.3. Data processing

Data was processed in three steps:

(1) quality check for the in-situ data

(2) MERIS and in-situ data which coincided were considered in the analysis ('match up stations').

(3) the validation process itself was carried out.

2.3.1. Quality control

All in-situ measurements taken into account fulfilled the following quality requirements:

- nearly clear sky
- wind speed < 10 m/s
- minimum of incoming solar light: $E_d(480\text{nm}) > 20 \frac{\text{mW}}{\text{m}^2\text{nm}}$ (described in [3])
- not influenced by dusk or dawn: $\frac{E_d(470\text{nm})}{E_d(680\text{nm})} > 1$ (described in [3])
- corresponding pitch and roll-data (measured by ship's sensor) > 5°

As defined in the MERIS product, the in-situ water leaving reflectance was then calculated by:

$$\rho_w = \pi \frac{L_u - \rho_{as} L_s}{E_d} \tag{1}$$

where the air-sea interface reflection coefficient ρ_{as} was estimated to be constantly equal to 0.2.

2.3.2. Match up stations

MERIS data acquired within one day overpassing the in-situ data were considered and averaged (3 by 3 pixels). This lead to several possible collocations per in-situ measurement. Tab. 1 lists the measurement dates, the corresponding collocations and the dedicated MERIS flags.

Table 1. Collocations of in-situ- and MERIS-data

Date	Colloc.	MERIS flags	Comment
300408	1		Wrong in-situ
010508	1		Clouds
	2		Clouds
020508	1	H_Glint, PCD1_13	
	2	H_Glint, PCD1_13	
	3	PCD1_13	Clouds
030508	1	PCD1_13	Side of cloud
	2		
090508	1	H_Glint, PCD1_13	Wrong in situ
100508	1	H_Glint, PCD1_13	
	2	H_Glint, PCD1_13	
110508	1	H_Glint, PCD1_13	
	2	H_Glint, PCD1_13	Negative ρ_m
130508	1	H_Glint, PCD1_13	Negative ρ_m
	2		
150508	1		

Match-up stations with clouds visible in the MERIS image and obviously unrealistic high in-situ data were excluded from further analysis and validation as well as significantly negative MERIS remote sensing reflectance ρ_w (see Tab. 1).

The remaining match-up stations were divided into a set of "good" (highlighted in Tab. 1 in green font colour) and a set of "alternative" (Tab. 1: blue font) match-up stations because of their visual agreement with the MERIS data and their ambient conditions.

2.3.3. Validation Process

In order to validate MERIS remote sensing reflectance with collocated in-situ data, the spectra are plotted for each collocation and the corresponding relative deviation is calculated. For all five "good" and the three "alternative" match-up stations the plots are given in Fig. 4 and Fig. 5, respectively.

3. RESULTS AND DISCUSSION

There is a rather good agreement between in-situ (Fig. 4 blue graphs) and MERIS remote sensing reflectance (Fig. 4 green graphs) in short wavelengths. For longer wavelengths the in-situ ρ_w are higher than the corresponding MERIS ρ_m. This can be due to the air-sea interface reflection coefficient ρ_{as} that was estimated to be constant, but in fact is a function of wind speed [1] and wavelength [see Doerffer et all, this proceedings]. Another reason might be that the height of the instruments above the water was not considered. Also an overestimation of atmospheric correction for MERIS L2 data is possible.

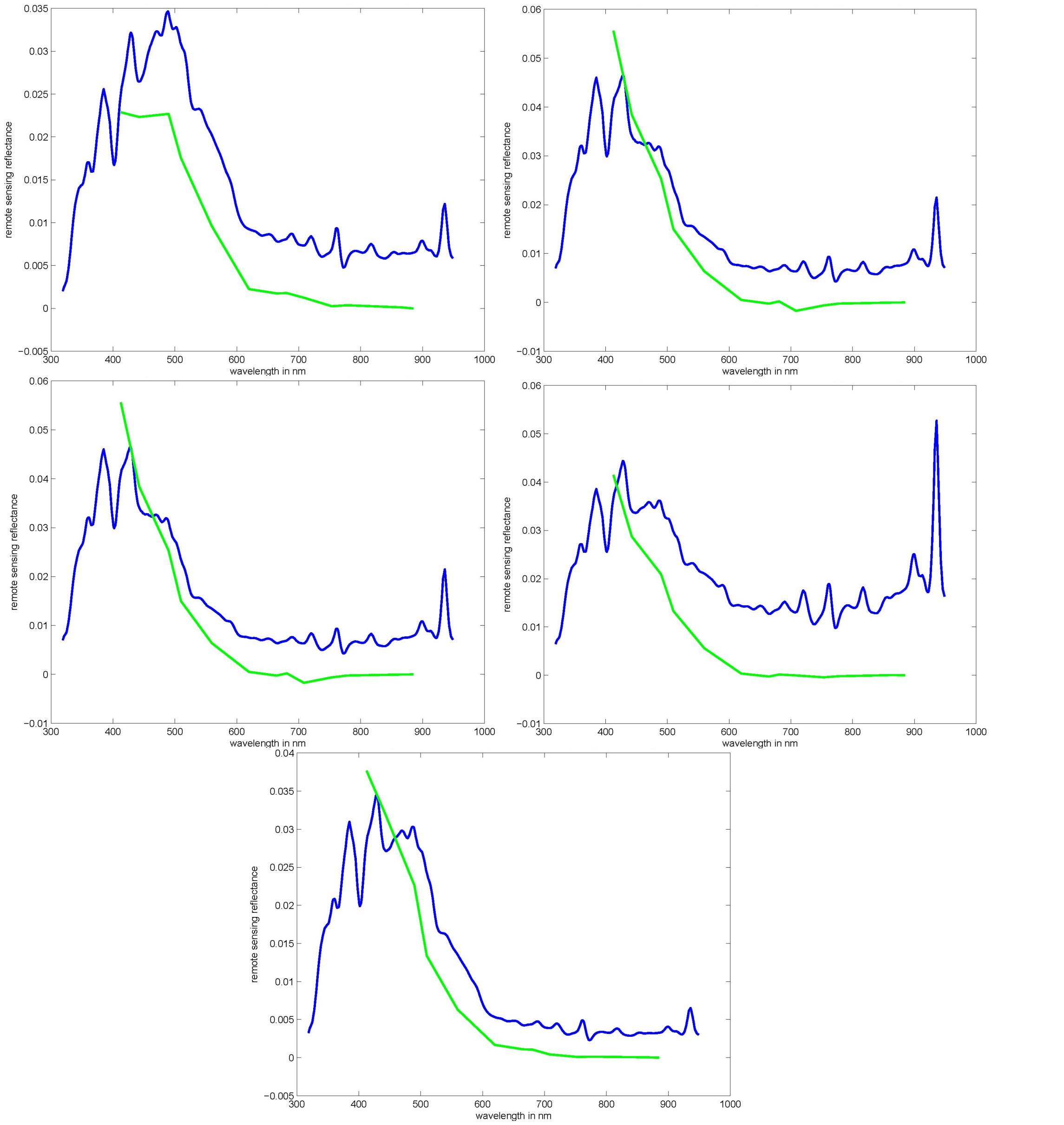

Figure 4. Comparisons of MERIS (green) and in-situ (blue) remote sensing reflectances as a function of wavelength for the five "good" match-up stations

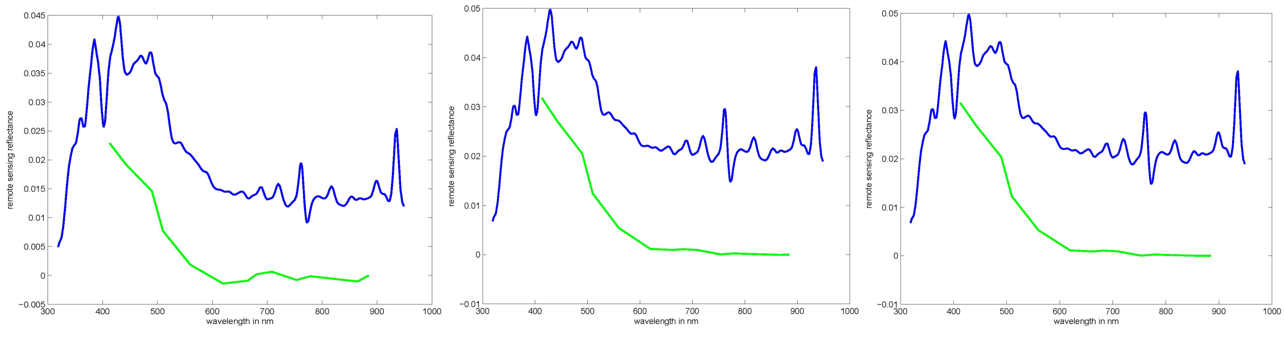

Figure 5. Comparisons of MERIS (green) and in-situ (blue) remote sensing reflectance as a function of wavelength for the three "alternative" match-up stations

The graphs for the “alternative” match up stations (Fig. 5) show a larger offset between the in-situ ρ_w and the MERIS ρ_m, what could be due to the rougher ambient conditions like larger wind speed.

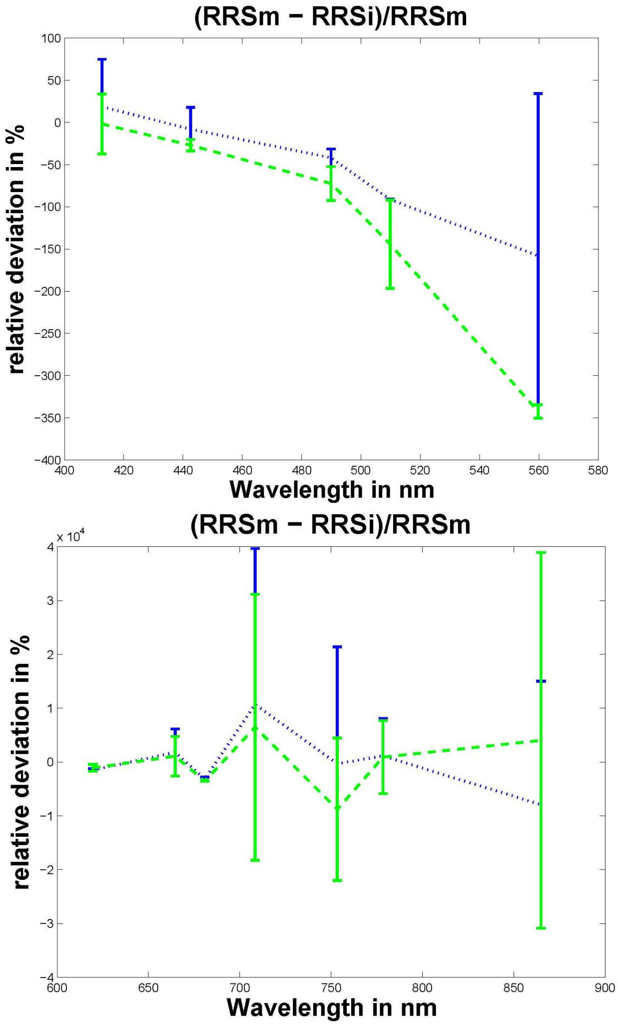

Figure 6. Relative deviation with 1-sigma intervals for good (blue) and alternative (green) data for smaller (above) and longer (below) wavelength ranges

After plotting the mean and the standard deviation of the relative deviations over all collocations are determined and plotted in Fig. 6. The analysis contains either only the good data (see Fig. 6 blue graph) or also the data set considering the good and the alternative data (see Fig. 6 green graph).

In general, the relative deviation and the standard deviation increase with wavelength, as can be seen in Fig. 6.
Taking the “alternative” match-up data with high glint and PCD1_13 in MERIS images into account, the standard deviation for most wavelengths is slightly increasing with respect to the standard deviation for only “good” match-up data, indicating that high glint flagged MERIS data are usable. It follows that the according threshold for high glint and PCD1_13 is too conservative.

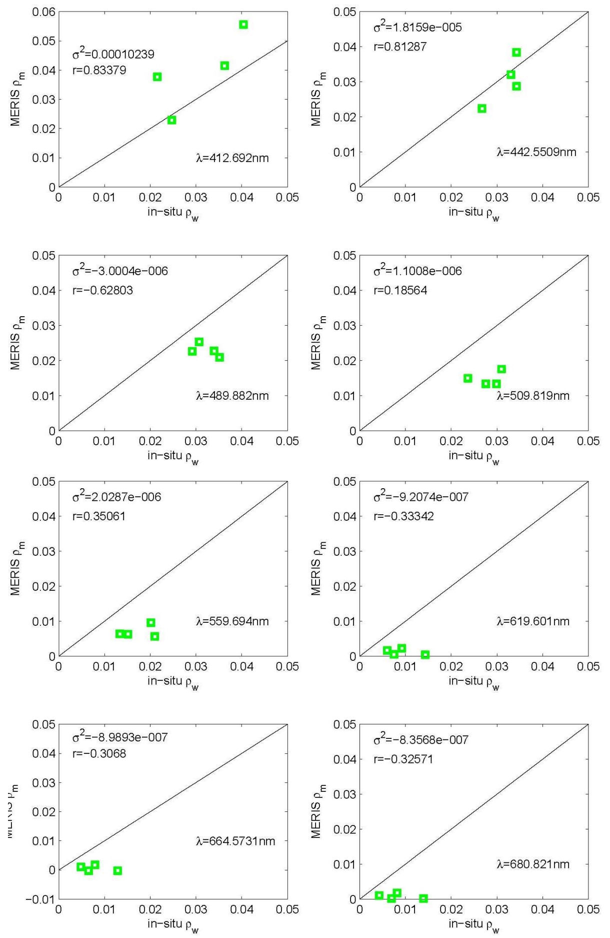

Figure 7. Scatterplots from MERIS versus in-situ remote sensing reflectance for the eight shortest MERIS wavelengths, indicated by λ in nm. *The corresponding covariance* σ^2 *and correlation coefficient r between MERIS* ρ_m *and in-situ* ρ_w *are shown in each subplot.*

Fig. 7 shows overall a better agreement at short wavelengths than at longer wavelengths: Shown are scatterplots from MERIS ρ_m versus in-situ ρ_w for the eight smallest MERIS wavelengths. The solid line in the plots is equal to the angel bisector and thereby is a visual reference for the agreement of both plotted vectors (MERIS ρ_m and in-situ ρ_w). The in-situ remote sensing reflectance is consequently larger than the MERIS remote sensing reflectance for long wavelengths. Possible reasons for that were discussed before.
Calculating the covariance and the correlation coefficient between both vectors gives a statistical quantity. For the two smallest wavelengths (413 nm and 443 nm) the correlation coefficient is nearest to one and

positive in contrast to the three largest wavelengths (620 nm, 665 nm and 680 nm) where the correlation coefficient is rather small and negative.
A linear fit between in-situ and satellite data is not performed due to the rather poor agreement for longer wavelength.

4. CONCLUSION AND OUTLOOK

Although improvements in flagging and atmospheric correction are needed in order to increase the usability of MERIS L2 data, it is also necessary to enhance in-situ data processing by considering the instrument‘s height above the water and adapt the air-sea interface reflection coefficient to the local conditions.
There will also be a validation of the MERIS L2-product chl a by calculating chl a concentration from in-situ data.
Finally, this validation process will be applied to data from other ship cruises across the Atlantic Ocean, such as RV Polarstern November 07 and November 08, RV M. S. Merian July – August 08, to get a comprehensive and consistent analysis of MERIS data quality.

5. ACKNOWLEDGEMENTS

We thank AWI and Helmholtz Impulse Fond for funding and ESA for delivering MERIS level-2 data and BEAM software. Our thanks also go to Wolfgang Schönfeld and Hajo Krasemann from GKSS, Wolfgang von Hoyningen-Huene and Tilman Dinter from IUP University of Bremen, Jill Schwarz from the National Institute of Water & Atmospheric Research (New Zealand) for data handling and Oliver Zielinski from Hochschule Bremerhaven for measurement devices.

6. REFERENCES

1. Park, Y., B. Van Mol, K. Ruddick (2006). Validation of MERIS water products for Belgian coastal waters 2002-2005. *Proceedings of the Second Working Meeting on MERIS and AATSR Calibration and Geophysical Validation (MAVT-2006)* 20-24 March 2006 ESRIN, Frascati, Italy
2. Ruddick, K.G., V. De Cauwer, Y.-J. Park (2006). Seaborne measurements of near infrared water-leaving reflectance: The similarity spectrum for turbid waters. *Limnol. Oceanogr., 51(2), 2006*, 1167-1179
3. Wernand, M.R. 2002. Guidelines for (ship-borne) auto-monitoring of coastal and ocean colour. Steven G. Ackleson-ONR, Charles Trees-NASA, Editors. Oceanographic Society. Ocean Optics XVI, Nov. 18-22, proceedings, Santa Fe, New Mexico, US
4. Antoine, D., F. d'Ortenzio, S. B. Hooker, G. Bécu, B. Gentili, D. Tailliez, A. J. Scott (2008). *Assessment of uncertainty in the ocean reflectance determined by three satellite ocean color sensors (MERIS, SeaWiFS and MODIS-A) at an offshore site in the Mediterranean Sea (BOUSSOLE project),* Journal of Geophysical Research, Volume 113, C07013, doi:10.1029/2007JC004472
5. Doerffer, R., H. Schiller, H. Krasemann, K. Heymann, W. Cordes, W. Schönfeld, R. Röttgers, I. Behner, P. Kipp (2003). *MERIS case 2 water validation – Early results North Sea / Helgoland / German Bight.* Proc. of Envisat Validation Workshop, Frascati, Italy, 9 – 13 December 2002 (ESA SP-531, August 2003)